Proteolytic Cleavage of the Fe−S Subunit Hinge Region of *Rhodobacter capsulatus* bc_1 Complex: Effects of Inhibitors and Mutations[†]

Maria Valkova-Valchanova,[‡] Elisabeth Darrouzet,[‡] Carolyn R. Moomaw,[§] Clive A. Slaughter,[§] and Fevzi Daldal*[,‡]

Department of Biology, Plant Science Institute, University of Pennsylvania, Philadelphia, Pennsylvania 19104, and Howard Hughes Medical Institute, Dallas, Texas, 75235

Received April 3, 2000; Revised Manuscript Received August 14, 2000

ABSTRACT: The three-dimensional structure of the mitochondrial bc_1 complex reveals that the extrinsic domain of the Fe−S subunit, which carries the redox-active [2Fe2S] cluster, is attached to its transmembrane anchor domain by a short flexible hinge sequence (amino acids D43 to S49 in *Rhodobacter capsulatus*). In various structures, this extrinsic domain is located in different positions, and the conformation of the hinge region is different. In addition, proteolysis of this region has been observed previously in a bc_1 complex mutant of *R. capsulatus* [Saribas, A. S., Valkova-Valchanova, M. B., Tokito, M., Zhang, Z., Berry E. A., and Daldal, F. (1998) *Biochemistry 37*, 8105−8114]. Thus, possible correlations between proteolysis, conformation of the hinge region, and position of the extrinsic domain of the Fe−S subunit within the bc_1 complex were sought. In this work, we show that thermolysin, or an endogenous activity present in *R. capsulatus*, cleaves the hinge region of the Fe−S subunit between its amino acid residues A46-M47 or D43-V44, respectively, to yield a protease resistant fragment with a M_r of approximately 18 kDa. The cleavage was affected significantly by ubihydroquinone oxidation (Q_o) and ubiquinone reduction (Q_i) site inhibitors and by specific mutations located in the bc_1 complex. In particular, using either purified or detergent dispersed chromatophore-embedded *R. capsulatus* bc_1 complex, we demonstrated that while stigmatellin blocked the cleavage, myxothiazol hardly affected it, and antimycin A greatly enhanced it. Moreover, mutations in various regions of the Fe−S subunit and cyt *b* subunit changed drastically proteolysis patterns, indicating that the structure of the hinge region of the Fe−S subunit was modified in these mutants. The overall findings establish that protease accessibility of the Fe−S subunit of the bc_1 complex is a useful biochemical assay for probing the conformation of its hinge region and for monitoring indirectly the position of its extrinsic [2Fe2S] cluster domain within the Q_o pocket.

The bc_1 complex [ubihydroquinone (QH_2)-cytochrome (cyt) *c* oxidoreductase][1] is a vital component of photosynthetic and respiratory electron transport pathways in mitochondria and bacteria (*1*−*4*). This integral membrane protein catalyzes oxidation of QH_2 and reduction of cyt *c* and converts the free-energy difference between these components to a membrane potential and a pH gradient, which are used subsequently for ATP synthesis. The structurally simplest form of the bc_1 complex is encountered in bacteria, including *Rhodobacter capsulatus* (*4*). It is composed of three subunits, the Fe−S subunit with a [2Fe2S] cluster, the cyt *b* with two *b*-type hemes (b_H and b_L), and the cyt c_1 with a *c*-type heme as prosthetic groups, and encoded by the *pet*A (*fbc*F), *pet*B (*fbc*B), and *pet*C (*fbc*C) genes, respectively (*1*, *4*). The three-dimensional structure of the bc_1 complex has been solved recently (*5*−*8*). The Fe−S subunit is composed of an amino terminal membrane anchor (residues 1−66 in bovine numbering, corresponding to 1−42 in *R. capsulatus*), a carboxyl terminal extrinsic domain (residues 74−196 corresponding to 50− 191 *in R. capsulatus*), and a short flexible hinge region (residues 67−73 corresponding to 43−49 in *R. capsulatus*) connecting them (Figure 1).

The modified Q cycle mechanism that relies on the presence of two separate quinone binding (Q_o and Q_i) domains as catalytic sites describes how the bc_1 complex functions (*9*−*11*). The Q_o site where the oxidation of QH_2 takes place is located near the periplasmic side, and the Q_i site, which is associated with ubiquinone (Q) reduction, is located on the cytoplasmic side of the membrane. This catalytic mechanism envisions efficient bifurcation of electrons emanating from the oxidation of QH_2 at the Q_o site. One of the electrons is transferred to the high potential chain composed of the Fe−S subunit and cyt c_1, and the other one is used to reduce initially the low potential heme b_L and then the high potential heme b_H and $Q/Q^{\bullet -}$ at the Q_i site (*11*−*13*). A long-range movement of the extrinsic domain carrying

[†] This work was supported by NIH Grant GM 38237 to F.D.

* To whom correspondence should be addressed. Phone: (215) 898-4394. Fax: (215) 898-8780. E-mail: fdaldal@sas.upenn.edu.

[‡] University of Pennsylvania.

[§] Howard Hughes Medical Institute.

[1] Abbreviations: cyt, cytochrome; bc_1 complex, ubihydroquinone-cytochrome *c* oxidoreductase; b_H, high potential *b*-type heme; b_L, low potential *b*-type heme; DPA, diphenylamine; E_m, redox midpoint potential; E_{m7}, redox midpoint potential at pH 7; EPR, electron paramagnetic resonance; DBH_2, 2,3-dimethoxy-5-methyl-6-decyl-1,4-benzohydroquinone; EDTA, ethylenediaminetetraacetic acid; MOA, E-β-methoxyacrylate; MOPS, 3-(N-morpholino)propanesulfonic acid; TMBZ, tetramethylbenzidine; PMSF, phenylmethylsulfonyl fluoride; Ps, photosynthesis; Q_o, ubihydroquinone oxidation site; Q_i, ubiquinone reduction site; Res, respiration; SDS−PAGE, sodium dodecyl sulfate−polyacrylamide gel electrophoresis; UHDBT, 5-*n*-undecyl-6-hydroxy-4,7-dioxobenzothiazole; [2Fe2S], two iron-two sulfur cluster.

10.1021/bi000751d CCC: $19.00
Published on Web 11/23/2000

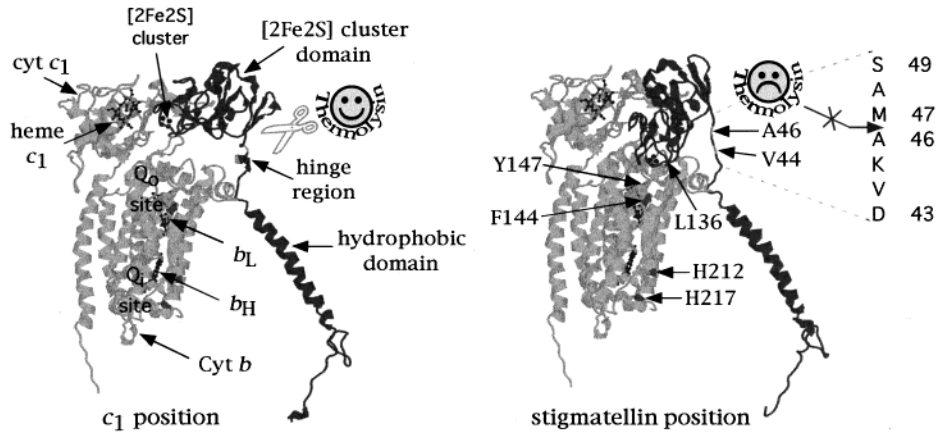

FIGURE 1: Three-dimensional structures of the chicken mitochondrial bc_1 complex crystallized in the absence of inhibitor (left) or in the presence of stigmatellin (right). Only the three catalytic subunits, the Fe−S subunit (in dark gray) and the cytochromes *b* and c_1 (in gray), with their respective prosthetic groups, the [2Fe2S] cluster, hemes b_L, b_H, and c_1 (in black) are indicated. The positions of the Q_o and Q_i catalytic sites, and the location of the Fe−S mutations V44, A46, and L136, and cyt *b* mutations F144, Y147, H212, and H217 are shown. The two different conformations of the hinge region when the extrinsic domain of the Fe−S subunit is in the c_1 or stigmatellin positions, its amino acid sequence between the positions 43 and 49 (*R. capsulatus* numbers), and the cleavage site of thermolysin (A46-M47) are also shown.

the [2Fe2S] cluster of the Fe−S subunit has recently been put forward as a component of this unusual bifurcation reaction at the Q_o site (*6*, *7*). This stems from the findings that in various mitochondrial bc_1 complex structures the position of the Fe−S subunit extrinsic domain changes with the presence of different Q_o site inhibitors, and also with different crystal forms (*5*−*8*). In particular, binding of stigmatellin or UHDBT locks the extrinsic [2Fe2S] cluster domain of the Fe−S subunit 27 Å away from heme b_L and 31 Å from heme c_1 (stigmatellin position) while that of MOA-stilbene moves this metal cluster closer to cyt c_1 (c_1 position) (Figure 1) (*8*). Crystallographic data also reveals that although the position of the extrinsic domain of the Fe−S subunit changes within the bc_1 complex, yet its overall conformation remains mainly unchanged and its transmembrane anchor domain stays fixed (*6*, *7*). Thus, the movement of the extrinsic domain is apparently accommodated by conformational changes of the flexible hinge region that are readily seen between the native and stigmatellin-containing bc_1 complex structures (Figure 1). Tian et al. (*14*) have shown using *Rhodobacter sphaeroides* that increasing the rigidity of the hinge region by mutating its highly conserved amino acids residues perturbs the activity of the bc_1 complex. We have also undertaken a detailed investigation of the role of this hinge region of *R. capsulatus* Fe−S subunit in Q_o site catalysis (*1*, *15*−*17*). The data obtained demonstrated that not only the flexibility, but also the length of the hinge region of the Fe−S subunit is a crucial parameter for the function of the bc_1 complex (*15*−*17*).

Earlier studies have indicated that the hinge region of the Fe−S subunit is sensitive to proteolytic cleavage with various proteases, including thermolysin (*18*−*20*). Proteolytic digestion of the mitochondrial bc_1 complex yields a protease-resistant form of the Fe−S subunit corresponding to its extrinsic [2Fe2S] cluster domain (*18*). A similar proteolysis has also been observed with the bacterial enzyme in a mutant of *R. capsulatus* (*21*). In the case of thermolysin, or the *R. capsulatus* mutant, this proteolytic cleavage occurs at position M71, or V68, of the mitochondrial Fe−S subunit, respectively (bovine numbering, corresponding *in R. capsulatus* to position M47 and V44, respectively), right within the hinge region. We therefore investigated whether the proteolytic sensitivity of this region changed in function of its conformation, and whether this proteolysis correlated with various positions of the extrinsic domain of the Fe−S subunit within the Q_o pocket.

In this work, we first establish that digestion of purified or detergent dispersed membrane-embedded bc_1 complex with thermolysin, or with a proteolytic activity endogenous to *R. capsulatus*, induces cleavage of the hinge region of the Fe−S subunit to a protease-resistant fragment with a M_r of approximately 18 kDa. We then demonstrate that this cleavage is blocked in the presence of the Q_o site inhibitor stigmatellin, but enhanced by the Q_i site inhibitor antimycin A. Thus, absence of proteolysis correlates with the stigmatellin position of the extrinsic domain of the Fe−S subunit at the Q_o pocket as seen in the structures of the bc_1 complex. Moreover, we show that different Q_o and Q_i site mutants carrying mutations located on various parts of the Fe−S subunit or cyt *b* change drastically this proteolysis pattern. Therefore, protease sensitivity of the hinge region of the Fe−S subunit in combination with various inhibitors and mutations reveals indirectly the position of its extrinsic [2Fe2S] cluster domain within the Q_o pocket of the bc_1 complex.

MATERIALS AND METHODS

Bacterial Strains and Growth Conditions. Wild-type and mutants *R. capsulatus* strains were grown chemoheterotrophically at 35 °C in MPYE enriched medium, supplemented with appropriate antibiotics and shaken in the dark at 150 rpm on a rotary shaker as described in ref *22*. The *R. capsulatus* parental strains pMTS1/MT-RBC1 and pMT0−404/MT-RBC1 overproduce the bc_1 complex by about 5−8-fold under these growth conditions. The mutants used in this work were derivatives of these strains (*23*−*27*), and their properties are listed in Table 1.

Chromatophore and Sphaeroplast Membranes Preparation and Purification of the bc_1 Complex. Chromatophore membranes were prepared as described in ref *22*, except that fresh cell pastes were resuspended at a ratio of 1−10 (w/v) in 50

Table 1: *R. capsulatus* Mutants Analyzed by Proteolytic Cleavage of the Hinge Region of Their Fe−S Subunit

strain	location of the mutation	Ps phenotype[a]	response to stigmatellin[b]	DBH_2:cyt *c* reductase activity (%)[c]	E_{m7} of the [2Fe2S] (mV)	refs
V44L	Fe−S subunit (hinge domain)	Ps^+	+	70	385	*25*
A46T	Fe−S subunit (hinge domain)	Ps^+	+	80	385	*25*
L136G	Fe−S subunit (extrinsic domain)	Ps^-	±	4	196	*24, 25*
L136A	Fe−S subunit (extrinsic domain)	Ps^+	±	26	310	*25*
Y147A	cyt *b* Q_o site	Ps^-	+	13	310	*27*
Y147S	cyt *b* Q_o site	Ps^-	+	14	310	*27*
Y147V	cyt *b* Q_o site	Ps^+	+	23	310	*27*
F144R	cyt *b* Q_o site	Ps^-	±	nd	290	*26*
H217R	cyt *b* Q_i site	Ps^+	+	60	nd[d]	*23*
H217D	cyt *b* Q_i site	Ps^+	+	60	nd	*23*
H212N	cyt *b* heme b_H	Ps^-	+	nd	nd	unpub[e]

[a] Ps^+ and Ps^- indicate photosynthetic competence and incompetence, respectively. [b] (+) The mutants are able to respond to stigmatellin, and (±) they respond to it differently than a wild-type strain as indicated by the shape of their EPR g_x signal. [c] The bc_1 complex enzymatic activity is expressed as a percentage of that found in a wild-type strain. [d] nd, not done. [e] unpub, K. Gray and F. Daldal, unpublished data.

mM Tris-HCl (pH 8.0) containing 100 mM NaCl, 1 mM PMSF, and 1 mM EDTA. Cells were broken by two passages through a French pressure cell at 18 000 psi. Membranes were washed thrice with 50 mM Tris-HCl (pH 8.0) and 100 mM NaCl and used for various biophysical measurements or purification of the bc_1 complex as described previously (*28*). Chromatophore membranes to be used for thermolysin assays were prepared in the presence of 17 mM EDTA to inhibit the endogenous proteolytic activity and washed extensively before use. Sphaeroplasts were prepared using a cell paste (2 g wet weight/50 mL) resuspended in 50 mM Tris-HCl (pH 8.0) containing 25% sucrose, 2 mM EDTA, and 0.1 vol of lysozyme (10 mg/mL), and incubated for 1 h at 4 °C. They were pelleted at 12000*g* for 25 min, resuspended in 10 mL of 10 mM Tris-HCl (pH 8.0) containing 15 mM $MgCl_2$ and 1 mg/mL DNAse, sonicated twice for 10 s using a Dynatech sonicator at an output of 2, and centrifuged at 12000*g* for 20 min to eliminate cell debris. The supernatant was then centrifuged at 120000*g* for 35 min. The sphaeroplast membranes thus pelleted were washed twice with 50 mM Tris-HCl (pH 8.0) and resuspended in the same buffer to a protein concentration of 30 mg/mL.

Proteolysis Assay Using Thermolysin. For thermolysin digestion, 0.6−0.75 nmol of purified bc_1 complex resuspended in 50 mM Tris-HCl (pH 8.0) and 100 mM NaCl were incubated for 5−10 min at room temperature with appropriate amounts of the bc_1 complex inhibitors as needed. The assay mixture contained 50 mM Tris-HCl (pH 8.0), 5 mM $CaCl_2$, 100 mM NaCl, and variable amounts of thermolysin from a stock solution of 0.0175−3.5% (w/v) in DMSO which corresponds to a concentration of 5.6 μM to 1.13 mM using a MW of 34 000 for thermolysin. The proteolysis assay was performed in a total reaction volume of 50 μL, and incubated at room temperature. Aliquots of 5−10 μL were withdrawn at specific time points, protease digestion was stopped by bringing up to 10 mM the final EDTA concentration, and samples were subjected to SDS−PAGE/immunoblot analyses. Membrane blots thus generated were scanned using an AlphaImager 950 system. The amount of the 18 kDa truncated Fe−S subunit was determined by densitometry analysis using the NIH Image software, and expressed as a percentage of the total amount of the Fe−S subunit (18 kDa + 24 kDa) per aliquot used. These experiments were repeated at least three times under linear response conditions, and a variation of 10−20% was found between the duplicates. Thermolysin assay conditions for membrane-embedded bc_1 complexes were essentially identical to those used for purified bc_1 complexes, except that prior to digestion chromatophore membranes (650 μg in 50 μL of 50 mM Tris-HCl, pH 8.0, buffer containing 100 mM NaCl) were incubated with 1 mg of dodecyl maltoside/mg of total protein for 1 h at room temperature.

Other Biochemical Assays and Analytical Measurements. Protein concentrations were determined by the method of Lowry et al. (*29*) using bovine serum albumin as a standard, and 15% SDS−PAGE was performed according to Laemmli (*30*). For immunoblot analyses, polyacrylamide gels were blotted onto Immobilon P-membranes (Millipore, Inc.), and polyclonal antibodies raised against the Fe−S subunit of *R. capsulatus* bc_1 complex were used (*22*). Horseradish peroxidase-conjugated anti-rabbit secondary antibodies (Bio-Rad) and metal ion enhanced diaminobenzidine (DAB) staining were used to detect the immune complexes. Amino terminal amino acid sequence determination was performed as described previously (*31*). Steady-state enzymatic activity of the bc_1 complex was assayed by measuring DBH_2-dependent reduction of horse heart cyt *c* as described in Atta Asafo-Adjei and Daldal (*22*).

Chemicals. Thermolysin and antimycin A were purchased from Sigma, and myxothiazol and stigmatellin from Fluka. Dodecyl maltoside was from Anatrace Inc., and duroquinone from Aldrich. The bc_1 complex inhibitors, tridecylstigmatellin, MOA-stilbene, and atovaquone were gifts from Drs. T. Wiggins, G. Hoefle, and A. Vaidya, respectively. DEAE-BioGel A and DEAE-Fractogel (Toyopearl-650) were obtained from Bio-Rad and EM Separation Technologies, respectively. All other chemicals were of reagent grade or of highest quality commercially available.

RESULTS

Thermolysin-Mediated Proteolytic Cleavage of the Fe−S Subunit of Purified bc_1 Complex. The Fe−S subunit was cleaved to an approximately 18 kDa fragment when purified

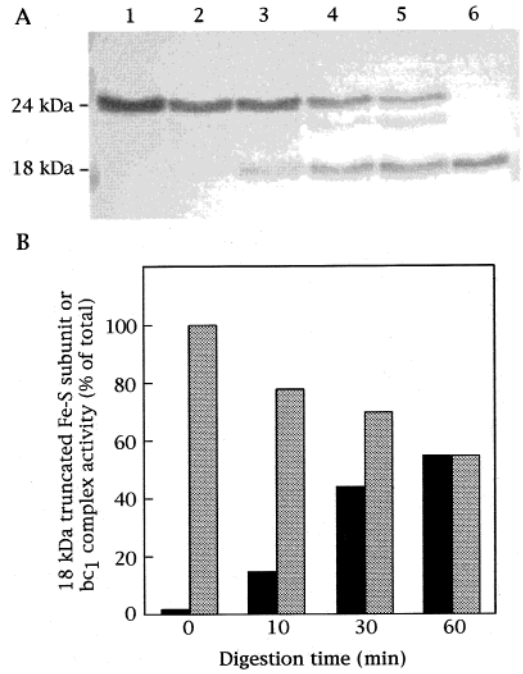

FIGURE 2: Thermolysin mediated proteolysis of purified *R. capsulatus* bc_1 complex. A total of 0.75 nmol of bc_1 complex were incubated at room temperature with 2 nmol of thermolysin in a total reaction volume of 50 μL, as described in Materials and Methods. Aliquots were removed at indicated time points (panel A, lanes 2−5, corresponding to 0, 10, 30, and 60 min), appearance of the 18 kDa truncated Fe−S subunit was monitored by SDS−PAGE/immunoblot analyses, and steady-state bc_1 complex activity was measured (panel B) as described in Materials and Methods. Lane 1 and 6 correspond to undigested purified bc_1 complex and purified 18 kDa truncated Fe−S subunit (*21*), respectively, used as controls. Black and gray bars indicate the amount of the 18 kDa band and the activity of the bc_1 complex, respectively. The experiments were repeated at least three times, and an average variation of 10−20% was seen between different experiments. The mean values for the 18 kDa truncated Fe−S subunit are presented as a percentage of the total amount of the Fe−S subunit (24 plus 18 kDa bands) present in each aliquot. For the bc_1 complex activity 100% corresponds to that found at zero min immediately after addition of thermolysin, and in this particular instance is 4.5 μmol of cyt *c* reduced min^{-1} mg of $protein^{-1}$, which is approximately 10 fold lower than untreated samples.

R. capsulatus bc_1 complex was digested with thermolysin under the assay conditions described in Materials and Methods (Figure 2A). The amount of this fragment, which was resistant to further proteolysis, increased with the incubation time while the total activity of the bc_1 complex decreased rapidly (Figure 2B). Determination of the amino-terminal amino acid sequence of the 18 kDa fragment after its immunoprecipitation using polyclonal antibodies against the *R. capsulatus* Fe−S subunit and SDS−PAGE indicated that thermolysin cleaved between the residues A46 and M47 of the native *R. capsulatus* Fe−S subunit (Figure 1). This cleavage site is located within the flexible hinge region of this protein connecting its extrinsic domain that carries its [2Fe2S] cluster and its hydrophobic membrane anchor. In these assays, no cleavage product(s) corresponding to the smaller amino terminal portion of the Fe−S subunit was detected, although occasionally, additional polypeptides of M_r larger than the 18 kDa fragment were seen. As expected, use of increasing amounts (from 0.01 to 2 nmol) of thermolysin/0.75 nmol of bc_1 complex increased the rate of cleavage, but under the assay conditions used here, at best, 50−60% of the available amount of the Fe−S subunit were cleaved in 60 min. Moreover, in no instance, even upon prolonged incubation (up to 20 h) or readdition of fresh thermolysin was the digestion complete. This indicated that purified bc_1 complexes contained, or yielded during the assay, a thermolysin resistant form of the Fe−S subunit. The molecular nature of the latter species was not investigated further.

Effect of the bc_1 Complex Q_o and Q_i Site Inhibitors on the Proteolytic Cleavage of the Fe−S Subunit. Considering that the different bc_1 complex inhibitors induce different positions for the extrinsic domain of the Fe−S subunit in various crystals (*5*−*8*), their effects on thermolysin-mediated cleavage of this subunit were investigated using purified *R. capsulatus* bc_1 complex. The presence of the Q_o site inhibitor stigmatellin (40-fold molar excess) blocked almost completely the proteolytic cleavage of the Fe−S subunit, while the Q_i site inhibitor antimycin A greatly enhanced it (Figure 3A). On the other hand, myxothiazol, which also inhibits Q_o site catalysis, did not appreciably affect the rate of thermolysin-mediated cleavage. Remarkably, the presence of antimycin A significantly decreased (from 40−50% to 20−30%) the fraction of the Fe−S subunit that was refractory to thermolysin digestion. Extension of these experiments to other known Q_o and Q_i site inhibitors established that UHDBT (at pH 6.5) (*32*) and HQNO behaved like stigmatellin and antimycin A, respectively (Figure 3B). On the other hand, mucidin (strobilurin A) acted like myxothiazol and tridecylstigmatellin (*33*), atovaquone (*34*), diphenylamine (DPA) (*35*), or the simultaneous presence of the Q_o and Q_i inhibitors exhibited intermediate effects.

The enhanced proteolysis seen with the Q_i site inhibitors antimycin A and HQNO was unexpected for their binding domain is located far away from the Q_o pocket where the extrinsic domain and the hinge region of the Fe−S subunit resides (*5*). This cleavage was therefore further analyzed using time-course experiments in the presence of various amounts of antimycin A and thermolysin. Both with 0.01 and 2 nmol of thermolysin/0.6 nmol of bc_1, increasing the amounts of antimycin A (from 0 to 50 nmol) induced increased rates of cleavage and amounts of the 18 kDa truncated Fe−S subunit.

Proteolytic Cleavage of the Fe−S Subunit of the bc_1 Complex in Chromatophores. To determine whether thermolysin digestion assays could also be performed with membrane-embedded, instead of purified bc_1 complexes, chromatophore, or sphaeroplast membranes were used. When these preparations were treated with thermolysin the Fe−S subunit remained intact unless the membranes were previously dispersed with dodecyl maltoside (Figure 4 panels A and B, lanes 2 and 4). Unexpectedly, control experiments using detergent solubilized chromatophores without thermolysin also produced an 18 kDa fragment of the Fe−S subunit (Figure 4A, lanes 3). Subsequent studies indicated that this was due to a proteolytic activity which is endogenous to *R. capsulatus* and sensitive to EDTA (Figure 4C, lane 1 and also see below). Thus, chromatophore membranes to be used for thermolysin digestions were prepared by breaking cells in the presence of 17 mM EDTA which was subsequently eliminated by extensive washes. Using such preparations, thermolysin treatment produced in a time-

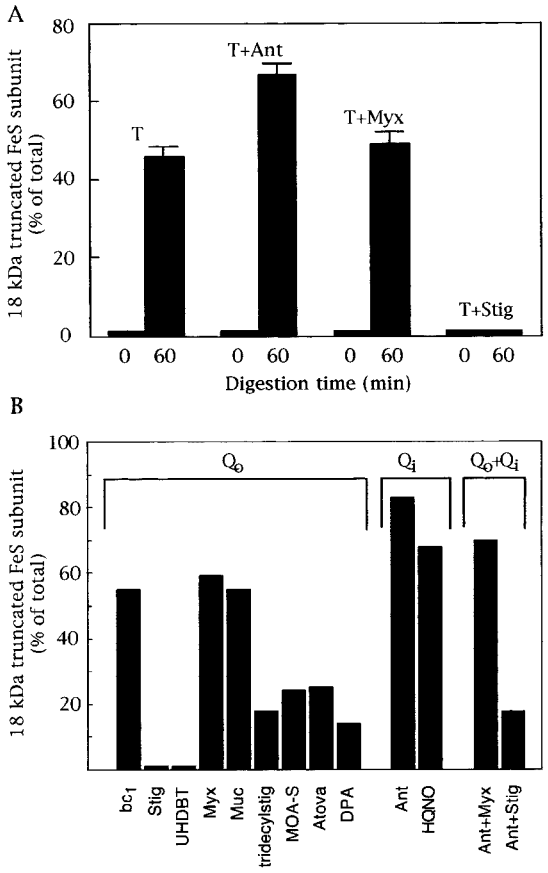

FIGURE 3: Thermolysin mediated proteolysis of purified *R. capsulatus* bc_1 complex in the presence of various bc_1 complex inhibitors. In panel A, 0.75 nmol of bc_1 complex was incubated with 2 nmoles of thermolysin (T) and in the presence of 30 nmoles (40-fold excess) of antimycin A (Ant), myxothiazol (Myx), or stigmatellin (Stig) under the experimental conditions described in Figure 2. The panel shows the bar graph indicating the amounts of the 18 kDa truncated Fe−S subunit produced at 0 and 60 min, respectively, as well as the standard error. Panel B summarizes similar data obtained in the presence of various Q_o and Q_i sites inhibitors as indicated. bc_1, Stig, UHDBT, Myx, Muc, tridecylstig, MOA-S, Atova, DPA, Ant and HQNO refer to purified bc_1 complex in the absence of inhibitor, in the presence of stigmatellin, 5-*n*-undecyl-6-hydroxy-4,7-dioxobenzothiazole, myxothiazol, mucidin (strobilurin A), tridecylstigmatellin, E-β-methoxyacrylate-stilbene [3-methoxy-2(2-styryl phenyl)propenic acid-methylester], atovaquone, diphenylamine, antimycin A and 2-*n*-heptyl-4-hydroxyquinoline *N*-oxide, respectively. As above, 30 nmoles of each inhibitor with 0.75 nmoles of purified bc_1 complex and 2 nmoles of thermolysin in a total reaction volume of 50 μL are used in each case. The bar graphs are the average of at least three separate experiments.

dependent fashion an 18 kDa fragment similar to that seen with the purified enzyme, and it decreased drastically the activity of the bc_1 complex (Figure 5). After 30 min of protease digestion, about 40% of the Fe−S subunit was converted to an 18 kDa fragment while 30% of the bc_1 complex remained active. Using dodecyl maltoside-solubilized chromatophore membranes, the effects of the bc_1 complex inhibitors stigmatellin, myxothiazol and antimycin A on thermolysin-mediated proteolytic cleavage of the Fe−S subunit were identical to those seen using purified bc_1 complexes (data not shown). Therefore, the overall data established that chromatophore membranes could be used reliably instead of the purified bc_1 complexes to monitor thermolysin-mediated proteolysis of the Fe−S subunit.

Endogenous Proteolytic Activity Capable To Cleave the Fe−S Subunit of the bc_1 Complex Is Present in R. capsulatus. Chromatophore, but not sphaeroplast, membranes prepared using the *R. capsulatus* wild-type strain pMTS1/MT-RBC1 contained an endogenous protease activity that released an approximately 18 kDa truncated Fe−S subunit in the presence of dodecyl maltoside (Figure 4A, lane 3, and Figure 6). This proteolytic activity was similar to that of thermolysin both in the absence and presence of various bc_1 complex inhibitors (Figure 6A), and could be stimulated by the presence of both ATP (2.5 mM) and $ZnSO_4$ (2.5 mM) (Figure 6B). Besides, this protease was independent of the presence of the bc_1 complex, and was released from intact cells upon treatment with chloroform (not shown) (*36*). Indeed, incubation of purified bc_1 complex with chromatophore membranes of the bc_1-deletion mutant MT-RBC1 of *R. capsulatus*, or with the soluble fraction after chloroform shock led to the same 18 kDa truncated form. These findings suggested that it might be located in the periplasm, in agreement with its absence in washed sphaeroplast membranes (Figure 4B, lane 3). The exact cleavage site of the hinge region of the Fe−S subunit by the endogenous proteolytic activity was not defined directly by amino acid sequencing of the 18 kDa fragment produced. However, our earlier work suggested that the cleavage site may be identical to the D43-V44 site previously determined using the soluble form of the Fe−S subunit encountered during chromatophore preparations from the suppressor mutants of the cyt *b* T163F substitution (*21*).

Thermolysin-Mediated Proteolytic Cleavage of the Fe−S Subunit in Various bc_1 Complex Mutants of R. capsulatus. The ability to use chromatophore membranes, instead of purified bc_1 complexes, allowed us to rapidly screen various *R. capsulatus* bc_1 complex mutants using thermolysin mediated proteolysis assay. For this purpose, Fe−S subunit mutants that carry mutations in their flexible hinge region (V44 and A46) (*25*) or in their extrinsic domain (L136G and L136A) (*24*), and cyt *b* mutants with mutations located near the Q_o (F144R and Y147A, S, V) (*26*, *27*) and the Q_i (H212N, H217D, and R) (*23*) sites were chosen (Table 1 and Figure 1). Proteolysis assays were done as described in Materials and Methods using either thermolysin or the endogenous proteolytic activity, and yielded comparable results (Figure 7). The V44L and A46T substitutions, which are located within the hinge region of the Fe−S subunit, increased significantly its proteolytic cleavage above the level seen with the wild-type bc_1 complex (from 5% in the wild-type to over 25% in the mutants with thermolysin, and from 40% to over 75% with the endoprotease). Moreover, addition of antimycin A further enhanced the cleavage in these mutants, but stigmatellin could only block it partially despite their known sensitivity to this inhibitor (*25*). Thus, the hinge domain mutations V44L and A46T not only increased the E_m value of the [2Fe2S] cluster as reported earlier (*25*), but also increased protease sensitivity of the hinge region of the Fe−S subunit. On the other hand, the Fe−S subunit extrinsic domain mutants L136G and L136A exhibited wild-type-like proteolytic cleavage patterns both in the absence of inhibitor or in the presence of antimycin A. Stigmatellin was unable to block completely proteolysis in these mutants which are known to exhibit increased resistance to this inhibitor (*24*, *25*).

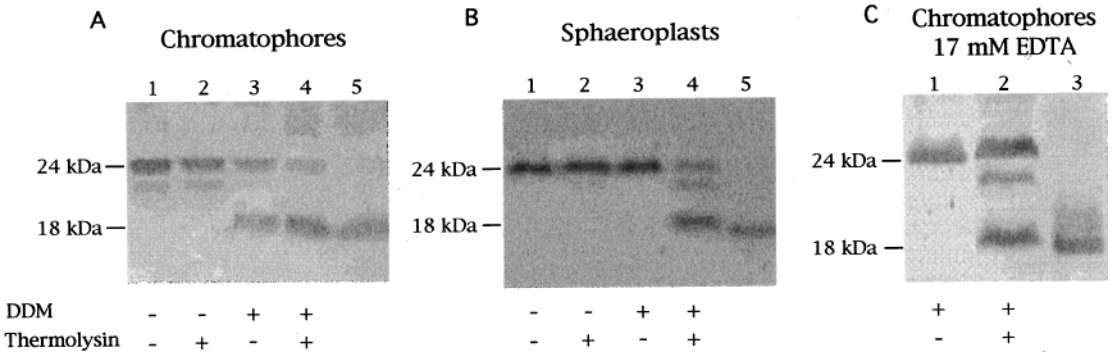

FIGURE 4: Digestion of membrane-embedded bc_1 complex from wild-type *R. capsulatus*. Chromatophore membranes (A), sphaeroplast membranes (B), or chromatophore membranes prepared in the presence of 17 mM EDTA (C) derived from pMTS1/MT-RBC1 were obtained as described in Materials and Methods. A total of 640 μg of these membranes were incubated for 60 min at room temperature in a 50 μL reaction mixture containing 0.5 nmol of thermolysin. (A and B) Lanes 1 and 2 correspond to nonsolubilized membranes in the absence (lane 1) and presence (lane 2) of thermolysin. Lanes 3 and 4 contain membranes incubated for 1 h with 1 mg of dodecyl maltoside (DDM)/mg of protein prior to digestion in the absence (lane 3) and presence (lane 4) of thermolysin. Lane 5 corresponds to the 18 kDa truncated Fe−S subunit used as a control. (C) Lanes 1 and 2 contain membranes prepared with 17 mM EDTA and solubilized with 1 mg of DDM/mg of protein prior to digestion in the absence (lane 1) and presence (lane 2) of thermolysin. Lane 3 corresponds to the 18 kDa truncated Fe−S subunit used as a control, as above.

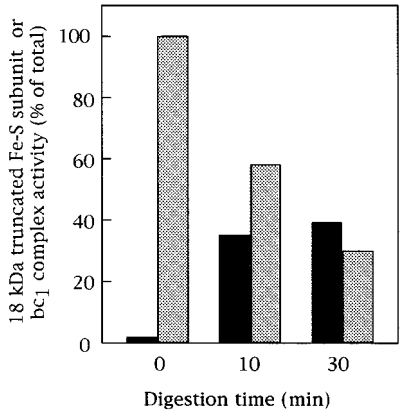

FIGURE 5: Thermolysin digestion of chromatophore membranes from wild-type *R. capsulatus*. Chromatophore membranes from pMTS1/MT-RBC1 were solubilized by 1 h incubation with 1 mg of dodecyl maltoside/mg of protein prior to thermolysin treatment, as described in Materials and Methods. A total of 650 μg of chromatophore membranes in a 50 μL reaction mixture were incubated at room temperature with 2 nmol of thermolysin for 10 or 30 min. Black and gray bars indicate the amount of the 18 kDa band and the activity of the bc_1 complex, respectively. All experiments were repeated at least three times, and the mean values obtained for the 18 kDa truncated Fe−S subunit are presented as a percentage of the total amount of the Fe−S subunit (24 kDa plus 18 kDa bands) present in each aliquot. For the bc_1 complex activity 100% corresponds to that found at zero min immediately after addition of thermolysin which was in this particular instance 0.4 μmol of cyt *c* reduced min^{-1} mg of membrane $protein^{-1}$, approximately 10-fold lower than untreated samples.

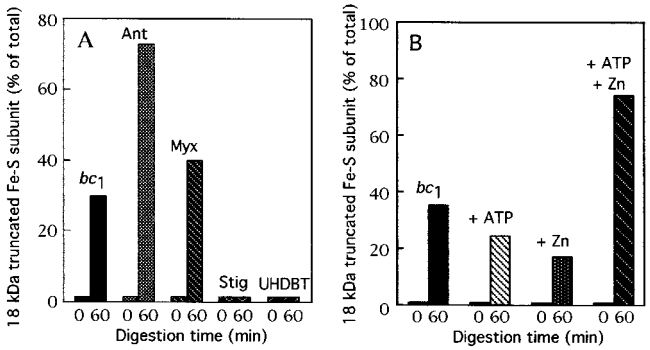

FIGURE 6: Proteolytic activity endogenous to *R. capsulatus* chromatophore membranes is able to cleave the Fe−S subunit of the bc_1 complex and is sensitive to Zn and ATP. (A) in a reaction mixture of 30 μL total volume 0.3 nmol of purified bc_1 complex was incubated in the presence of 30 nmol of antimycin A (Ant), myxothiazol (Myx), stigmatellin (Stig) or UHDBT, and compared to no inhibitor (bc_1). The incubation period was 60 min in each case, and the percentage of the 18 kDa fragment observed was plotted as a bar graph, as described in Figure 2 and in Materials and Methods. (B) experiments identical to those described in Panel A were performed, except that the digestion mixture contained ATP or Zn or both components as indicated, and the incubation period was for 60 min. bc_1, no addition; +ATP, in the presence of 2.5 mM ATP; +Zn, in the presence of 2.5 mM $ZnSO_4$ and +ATP+Zn, in the presence of 2.5 mM ATP and 2.5 mM $ZnSO_4$.

The cyt *b* mutants Y147A, S, and V were less sensitive to proteolysis of the hinge region of their Fe−S subunit both in the absence of inhibitor and in the presence of antimycin A (Figure 7). F144R behaved almost like a wild-type strain, but it responded only partially to inhibition by stigmatellin, probably due to the previously observed increased resistance to this inhibitor with the F144 substitutions (*26*). In any events, the cyt *b* mutants indicated that perturbation of the electron-transfer reactions at the Q_o site only slightly decreased the cleavage of the flexible hinge region of the Fe−S subunit. On the other hand, the cyt *b* H217D, R, and H212N substitutions altered more drastically the cleavage pattern of the Fe−S subunit which was hypercleavable even in the absence of antimycin A or in the presence of stigmatellin (Figure 7A). Thus, absence of an intact Q_i site (*23*) or heme b_H increased significantly protease sensitivity of the Fe−S subunit hinge region. In summary, the overall findings established that the changes induced by various bc_1 complex mutations and inhibitors on the position of the Fe−S subunit in the Q_o pocket can be monitored by probing the protease sensitivity of its hinge region.

DISCUSSION

In the present work, a biochemical assay that reports on the location of the extrinsic domain of the Fe−S subunit in the Q_o pocket was developed. This assay uses proteolysis with thermolysin or with an endogenous activity naturally present in *R. capsulatus* chromatophore membranes. These enzymes cleave within the flexible hinge region (between

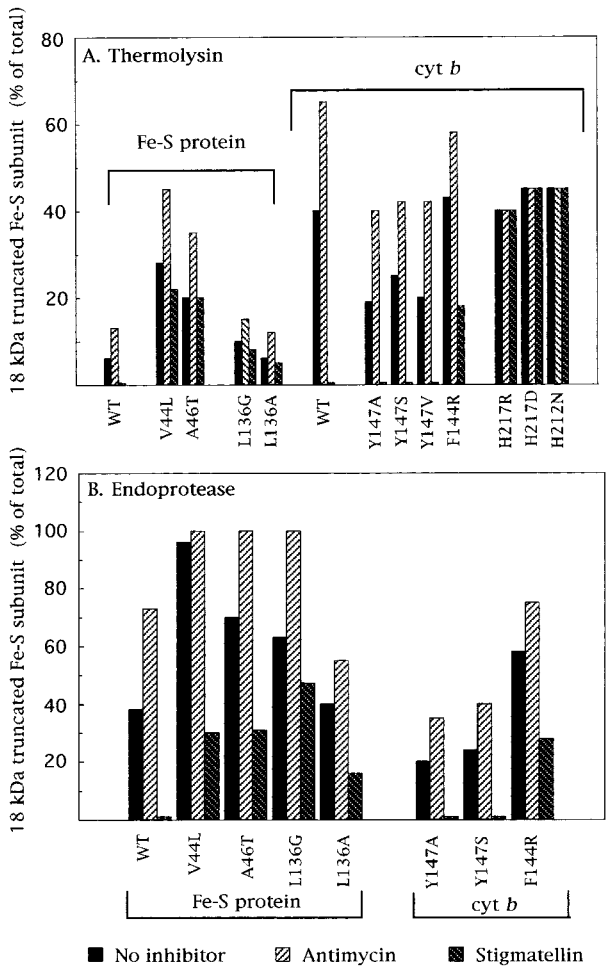

FIGURE 7: Proteolytic cleavage of the Fe−S subunit in dodecyl maltoside dispersed chromatophores derived from various *R. capsulatus* mutants. (A) thermolysin-mediated cleavage of the Fe−S subunit of the bc_1 complex in various Fe−S subunit and cyt *b* mutants (see Table 1 for their properties). A total of 650 μg of chromatophore membranes which were prepared in the presence of 17 mM EDTA, and solubilized with 1 mg dodecyl maltoside per mg of total protein, as described in Materials and Methods, were used. Thermolysin digestions were for 60 min, using either 0.01 nmol for the Fe−S subunit mutants or 0.2 nmol for the cyt *b* mutants, in the absence of inhibitor (first bar), in the presence of 30 nmol of antimycin A (second bar), or of stigmatellin (third bar) in each case. Digested samples were analyzed by immunoblot assays, the amounts of the 18 kDa truncated Fe−S subunit were quantitated as described in Materials and Methods, and plotted as bar graphs. In each case the values shown are the average of at least three separate experiments. Panel B corresponds to similar experiments as in panel A, and the digestions were carried out without thermolysin, either in the absence of inhibitor or in the presence of antimycin A or stigmatellin using dodecyl maltoside solubilized chromatophore membranes prepared in the presence of only 1 mM EDTA as described in Materials and Methods, thus exhibiting the endogenous proteolytic activity present in *R. capsulatus*.

the residues A46-M47 or D43-V44, respectively) of the Fe−S subunit of the bc_1 complex to yield a carboxyl terminal fragment of about 18 kDa M_r which is highly resistant to further degradation. They yield similar cleavage patterns in the presence or absence of various Q_o and Q_i site inhibitors and mutations. A variety of different proteases including trypsin (*18*, *19*), papain (*20*) and other serine proteases (*37*, *38*) also cleave within this region in both bacterial and mitochondrial bc_1 complexes. This suggests that the protease sensitivity of the Fe−S subunit is an intrinsic property of this subunit, and not specific to the species or the proteases used. Why the proteolysis is incomplete using purified bc_1 complex and why the Fe−S subunit of the membrane-embedded bc_1 complex is not sensitive to protease digestion in the absence of detergent dispersion are presently unclear. A similar situation has also been encountered with chromatophore and sphaeroplast membranes of *R. sphaeroides* treated with proteinase K, and detergent treatment of the cleavage site being necessary for its exposure to protease has been suggested (*39*).

Various bc_1 complex inhibitors affect proteolysis of the hinge region of the Fe−S subunit differently. Among the Q_o site inhibitors stigmatellin and UHDBT, which are known to raise the E_m of the [2Fe2S] cluster (*40*), block it almost completely while myxothiazol and MOA-stilbene do not interfere with it. Proteases, including thermolysin, are often sensitive toward the conformation of their substrates (*41*), suggesting that the protease resistance or sensitivity of the Fe−S subunit reflect the structural changes that take place in its flexible hinge region. Indeed, the structures of the mitochondrial bc_1 complexes that contain inhibitor (*5*−*8*) show that, in the presence of stigmatellin, the extrinsic domain of the Fe−S subunit is buried into cyt *b* close to heme b_L. In addition, the conformation of the hinge domain is converted from two turn helices to a random coil (Figure 1). The protease patterns found here suggest that UHDBT, which acts like stigmatellin, also induces conformational changes within the hinge region of the Fe−S subunit, while MOA-stilbene, which behaves like myxothiazol, does not. Similarly, reduced proteolysis seen with inhibitors such as atovaquone and DPA suggests that they have intermediate effects (*34*, *35*). It appears that the lack of cleavage of the hinge region of the Fe−S subunit is a reliable indicator for this conformational change, and reflects indirectly the location of its extrinsic domain when it occupies the stigmatellin position at the Q_o pocket. Conversely, proteolytic cleavage of the hinge region provides rather limited information about the location of the Fe−S subunit extrinsic domain for it is observed under many different Q_o site occupancy conditions, such as absence of inhibitor or presence of myxothiazol, where this domain is expected to occupy different locations.

An unexpected finding is the enhanced cleavage rate and amount of the hinge region of the Fe−S subunit in the presence of the antimycin A-like Q_i site inhibitors. The binding pocket of this inhibitor in the bc_1 complex is far away from the hinge region of the Fe−S subunit and from the various locations of its extrinsic domain in the Q_o pocket (Figure 1) (*5*−*8*). Further, available structural data do not reveal any pronounced conformational change in any part of the Fe−S subunit in the presence or absence of antimycin A (*6*). Moreover, our earlier work has demonstrated that elimination of this Fe−S subunit does not affect the properties of the Q_i site in respect to its interactions with antimycin A or its ability to stabilize the Q_i semiquinone (*28*). Yet, enhanced proteolysis of the Fe−S subunit suggests that the conformation or protease accessibility of this subunit change in the presence of antimycin A. Under these conditions, the extrinsic domain of the Fe−S subunit is still located in the Q_o pocket, as indicated by the EPR g_x signal as well as an unmodified E_m of the [2Fe2S] (data not shown).

This suggestion is further supported by the finding that antimycin A also enhances proteolytic cleavage even in the presence of stigmatellin which locks the extrinsic domain of the Fe−S subunit in the Q_o site. How antimycin A enhances proteolysis is unclear. In the dimeric structure of the bc_1 complex, the membrane anchor of the Fe−S subunit of one monomer is close to the Q_i site of the other monomer since they are intertwined (*5*−*8*). Thus, an intriguing possibility would be a conformational change of the hinge region of the Fe−S subunit via modifications of its membrane anchor in response to the Q_i site redox events at the other monomer, as seen with antimycin A or with various Q_i sites mutants. Whether such an intertwined dimeric structure is also the basis of the observed maximum 50% proteolytic cleavage of the hinge region of the Fe−S subunit during thermolysin treatment of purified native bc_1 complexes remains to be seen. In addition, it has also been observed that in the presence of antimycin A stability of the mitochondrial bc_1 complex is increased and degradation of its cyt *b* and cyt c_1 subunits are decreased (*38*). These findings again support the idea that structural modifications around the Q_i site upon binding of antimycin A induce conformational changes in the hinge region of the Fe−S subunit and modulate its protease sensitivity.

Analysis of various previously well-characterized mutants of the bc_1 complex (*23*−*27*) using the proteolysis assay developed here have yielded important information. First, it appears that among the mutants tested those with mutations at positions 44 and 46 of the hinge region of the Fe−S subunit exhibited enhanced proteolytic cleavage, while preserving their wild-type-like responses to stigmatellin or antimycin A. Presumably, in these mutants conformational changes at their hinge regions modify the equilibrium distribution of their Fe−S subunit at the Q_o pocket while they also increase the E_m values of the [2Fe2S] clusters (*25*). Second, at least some of the mutants defective in Q_o site catalysis, such as those tested here, affect only slightly the conformation of the hinge region, or the position of the Fe−S subunit at the Q_o site. These mutants carried mutations located either on the extrinsic domain of the Fe−S subunit (position L136, interacting directly with cyt *b* at the Q_o pocket), or within the Q_o domain of cyt *b* (at position 144, changing the Q_o site occupancy, or position 147, perturbing bifurcated electron transfer at the Q_o site) (Table 1). These observations further enhance the finding that a nonfunctional Q_o site does not necessarily perturb the movement of the Fe−S subunit as already revealed for example by the cyt *c* reduction kinetics of Y147A (*27*, and see ref *16* for more details). Moreover, the heme b_H ligand and Q_i site mutants located at positions 212 and 217 of cyt *b*, respectively, indicated that their hinge domain became hypersensitive to proteolysis even in the absence of antimycin A. Thus, these mutants may have already adopted a conformation similar to what occurs in the wild-type Fe−S subunit when exposed to the Q_i site inhibitors. According to the Q cycle mechanism, reduction of the hemes b_L and b_H should ready the Fe−S subunit to transfer to cyt c_1 the electron it had captured from QH_2 oxidation. This would require moving its extrinsic domain away from the stigmatellin position at the Q_o site where it is less prone to proteolysis, toward the c_1 position where its proteolytic vulnerability increases. Such a mechanistic interlink could then temporally coordinate the redox events that take place at the Q_o and Q_i sites. Analyses of additional mutants and inhibitors using the protease sensitivity of the Fe−S subunit should provide further information on this issue.

Neither the molecular nature nor the physiological function if any of *R. capsulatus* ATP and Zn stimulated proteolytic activity that cleaves specifically the hinge region of the Fe−S subunit are known. Moreover, whether this stimulatory effect is mediated by some regulatory action of ATP or Zn directly on the bc_1 complex or on the endogenous proteolytic activity is unknown. While Zn is known to inhibit the bc_1 complex activity (*42*, *43*) by binding to two sites located in the close vicinity of the Q_o site, as determined very recently by X-ray crystallography (E. Berry, personal communication), its mode of action is unknown. This inhibition could be caused by interference with the deprotonation events that take place during QH_2 oxidation, which would induce a conformational change in the bc_1 complex enhancing the cleavability of the hinge region of the Fe−S subunit. If this is the case, then future analysis of the effect of Zn on proteolysis may provide invaluable insights into the events linking the electron transfer, the movement of the Fe−S subunit, and the proton transfer during Q_o site catalysis.

REFERENCES

1. Darrouzet, E., Valkova-Valchanova, M., Ohnishi, T., and Daldal, F. (1999) *J. Bioenerg. Biomembr. 31*, 257−288.
2. Gennis, R. B., Barquera, B., Hacker, B., Van, D. S. R., Arnaud, S., Crofts, A. R., Davidson, E., Gray, K. A., and Daldal, F. (1993) *J. Bioenerg. Biomembr. 25*, 195−209.
3. Trumpower, B. L., and Gennis, R. B. (1994) *Annu. Rev. Biochem. 63*, 675−716.
4. Gray, K., and Daldal, F. (1995) in *Anoxygenic Photosynthetic Bacteria* (Blankenship, R. E. Madigan, M. T., and Bauer, C., Eds) Kluwer Academic Publishers, Dordrecht, The Netherlands, pp 747−774.
5. Xia, D., Yu, C.-A., Kim, H. Xia, Y. Z., Katchurin, A. M., Zhang, L., Yu, L. and Deisenhofer, J. (1997) *Science 277*, 60−66.
6. Zhang, Z., Huang, L., Shulmeister, V. M., Chi, Y.-I., Kim, K. K., Hung, L. W., Crofts, A. R., Berry, E. A., and Kim, S. H. (1998) *Nature 392*, 677−684.
7. Iwata, S., Lee, J. W., Okada, K., Lee, J. K., Iwata, M., Rasmussen, B., Link, T. A., Ramaswamy, S., and Jap, B. K. (1998) *Science 281*, 64−71.
8. Kim, H., Xia, D., Yu, C.-A., Kachurin, A. M., Zhang. L., Yu, L., and Deisenhofer, J. (1998) *Proc. Natl. Acad. Sci. U.S.A. 95*, 8026−8033.
9. Mitchell, P. (1976) *J. Theor. Biol. 62*, 327−367.
10. Croft, A. R., Meinhardt, S. W., Jones, K. R., and Snozzi, M. (1983) *Biochim. Biophys. Acta 723*, 202−218.
11. Ding, H., Robertson, D. E, Daldal, F., and Dutton, P. L. (1992) *Biochemistry 31*, 3144−3158.
12. Brandt, U. (1996) *FEBS Lett.* 387, 1−6.
13. Crofts, A. R., Barquera, B., Gennis, R. B., Kuras, R., Guergova-Kuras, M., and Berry, E. A. (1997) in *The Phototrophic prokaryotes* (Pescheck, G. A., Loeffelhardt, W., and Schmetterer, G., Eds) Kluwer Academic/Plenum Publisher, New York, pp 229−239.
14. Tian, H., Mather, M. W., and Yu, C.-A. (1998) *J. Biol. Chem. 273*, 27953−27959.
15. Darrouzet, E., Valchova-Valchanova, M., and Daldal, F. (1999) in *Photosynthesis: Mechanisms and Effects* (Garab, G., Ed.) Vol. 3, pp 312−316, Kluwer Academic Press, Dordrecht, The Netherlands.
16. Darrouzet, E., Valkova-Valchanova, M., Moser, C. C., Dutton, P. L., and Daldal, F. (2000) *Proc. Natl. Acad. Sci. U.S.A. 97*, 4567−4572.

17. Darrouzet, E., Valkova-Valchanova, M., and Daldal, F. (2000) *Biochemistry 39*, 15475−15483.
18. Link, T., Saynovits, M., Assmann, C., Iwata, S., Ohnishi, T., and Von Jagow, G. (1996) *FEBS Lett. 237*, 71−75.
19. Gonzalez-Halphen, D., Vazquez-Acevedo, M., and Garcia-Ponce, B. (1991) *J. Biol. Chem. 266*, 3870−3876.
20. Lorusso, M., Cocco, T., Boffoli., D., Gatti, D., Meinhardt, S., Ohnishi, T., and Papa, S. (1989) *Eur. J. Biochem. 179*, 535−540.
21. Saribas, A. S., Valkova-Valchanova, M., Tokito, M. K., Zhang, Z., Berry, E. A., and Daldal, F. (1998) *Biochemistry 37*, 8105−8114.
22. Atta-Asafo-Adjei, E., and Daldal, F. (1991) *Proc. Natl. Acad. Sci. U.S.A. 88*, 492−496.
23. Gray, K., Dutton, P. L., and Daldal, F. (1994) *Biochemistry 33*, 723−733.
24. Liebl, U., Sled, V., Brasseur, G., Ohnishi, T., and Daldal, F. (1997) *Biochemistry 36*, 11675−11684.
25. Brasseur, G, Sled, V., Liebl, U., Ohnihi, T., and Daldal, F. (1997) *Biochemistry 36*, 11685−11696.
26. Ding, H., Daldal, F., and Dutton, P. L. (1995) *Biochemistry 34*, 15997−16003.
27. Saribas, A. S., Ding, H., Dutton, P. L., and Daldal, F. (1995) *Biochemistry 34*, 16004−16012.
28. Valkova-Valchanova, M. B., Saribas, S. A., Gibney, B., Dutton, P. L., and Daldal, F. (1998) *Biochemistry 37*, 16242−16251.
29. Lowry, O. H., Rosenbrough, N. J., Farr, A. L., and Randall, R. J. (1951) *J. Biol. Chem. 193*, 265−275.
30. Laemmli, U. K. (1970) *Nature 227*, 680−685.
31. Myllykallio, H., Jenney, F. E., Moomaw, C., Slaughter, C. A., and Daldal, F. (1997) *J. Bacteriol. 179*, 2623−2631.
32. Meinhardt, S., Yang, X., Trumpower, B., Ohnishi, T. (1987) *J. Biol. Chem. 262*, 8702−8706.
33. Ohnishi, T., Brandt, U., and von Jagow, G. (1988) *Eur. J. Biochem. 116*, 385−389.
34. Srivastava, I. K., Morrisey, J. M., Darrouzet, E., Daldal, F., and Vaidya, A. B. (1999) *Mol. Microbiol. 33*, 704−711.
35. Sharp, R. E., Palmitessa, A., Gibney, B. R., White, J. L., Moser, C. C., Daldal, F., and Dutton, P. L. (1999) *Biochemistry 38*, 3440−3446.
36. Ames, G. F. L., Prody, C., and Kustu, S. (1984) *J. Bacteriol. 160*, 1181−1183.
37. Gonzalez-Halphen, D., Lindorfer, M. A., and Capaldi, R. A. (1988) *Biochemistry 27*, 7021−7031.
38. Rieske, J., Baum, H., Stoner, C. D., and Lipton, S. H. (1967) *J. Biol. Chem. 242*, 4854−4866.
39. Wu, J., and Niederman, R. A. (1995) *Biochem. J. 305*, 823−828.
40. von Jagow, G., and Ohnishi, T. (1985) *FEBS Lett. 185*, 311−315.
41. Kumigi, S., Fujiwara, S., Kidokoro, S., Endo, K., and Hanzawa, S. (1999) *FEBS Lett. 462*, 231−235.
42. Lorusso, M., Cocco, T., Sardanelli, A. M., Minuto, M., Bonomi, F., and Papa, S. (1991) *Eur. J. Biochem. 197*, 555−561.
43. Link, T. A., and von Jägow, G. (1995) *J. Biol. Chem. 270*, 25001−25006.
44. Robertson, D., Ding, H., Chelminski, P., Slaughter, C., Hsu, J., Moomaw, C., Tokito, M., Daldal, F. and Dutton, P. L. (1993) *Biochemistry 32*, 1310−1317.

BI000751D